ASTFE
American Society of Thermal and Fluids Engineers

3rd Thermal and Fluids Engineering Conference (TFEC)
March 4–7, 2018
Fort Lauderdale, FL, USA

TFEC-2018-21802

THE KEY ROLE OF PUMPING POWER IN ACTIVE COOLING SYSTEMS

Mohammad Reza Shaeri

Advanced Cooling Technologies, Inc., 1046 New Holland Avenue, Lancaster, PA 17601, USA

ABSTRACT

Active air-cooled heat sinks are among the most commonly used thermal management solutions in broad applications. Although reducing the thermal resistance of a heat sink is one of the main goals of developing an efficient heat sink, pressure drop across the heat sinks is another important parameter, as such high pressure drops may impede utilizing the heat sink regardless of its low thermal resistances. As a result, reporting thermal performance of a heat sink without pointing to its pressure drop would lead to confusion and uncertainty about the functionality of the heat sink in practical applications. In this study, the crucial role of pumping power in designing and selecting efficient heat sinks is demonstrated by performing experiments on perforated-finned heat sinks at five different porosities, and comparing the results with those of a heat sink without perforations. This study presents a practical insight about comparing the performances of different heat sinks, as well as a new family of efficient heat sinks.

KEY WORDS: Air-cooled heat sink, Thermal resistance, Pressure drop, Pumping power.

1. INTRODUCTION

The low cost, simplicity, and availability of air have made active air-cooled heat sinks the primary thermal management solutions in a variety of applications from microscale to large-sized systems [1]. These heat sinks consist of fans used to draw air through parallel channels that are separated from each other via fins. The heat source that is attached to the heat sink will be cooled by exchanging heat to the flowing air inside the channels [2]. Designing an efficient heat sink requires minimizing the key design parameters of (i) thermal resistance, (ii) pumping power, and (iii) volume [3]. Combining 85 KWh/kg that is required to form, assemble, and transport aluminium heat sinks with the energy consumed in the operation of the fans, the total energy required for the cooling of a typical microprocessor can be expressed as [4]:

$$E_{\mathrm{T}} = 85M + P_p t \qquad (1)$$

where E_{T} (KWh), M (kg), P_p (W), and t (hrs) are the energy used for cooling, mass of the heat sink, the fan pumping power, and the operating lifetime of the fan, respectively.

In this study, the key role of pumping power in designing and describing the thermal performances of air-cooled heat sinks is demonstrated by investigating the thermo-fluid characteristics of perforated-finned heat sinks (PFHSs) through experiments. The experimental setup and PFHSs are illustrated in Fig. 1. Comprehensive explanations about the experimental procedure are provided in references [1] and [5]. A centrifugal blower blew the air through a stainless steel duct with a rectangular cross section of 7.62 cm by 3.73 cm and a length of 1.5 m. The heat sinks were made of 6063-T5 aluminium alloy, and included 19 parallel channels (20 fins) with the fin thickness at 0.96 mm, and the channel length (L), height (H), and width (W_{ch}) at 203 mm, 22.86 mm, and 2.18 mm, respectively. The thickness of the heat sink base was at 2.54 mm. Square cross sectional perforations with the size (L_P) of 7.62 mm were fabricated on the lateral surfaces of the fins by

*Corresponding Author: mohammadreza.shaeri@1-act.com

EDM technique. All PFHSs had two rows of perforations. Five PFHSs were tested at different porosities, as such, the porosity of 0.15, 0.25, 0.35, 0.45, and 0.55 were equivalent to PFHSs with 12, 20, 28, 36, and 44 perforations, respectively. The porosity (ϕ) is defined as the ratio of the void volume of the fins due to perforations to the volume of the fin without perforation, as $\phi = \frac{N_P L_P^2}{HL}$, where N_P stands for the number of perforations.

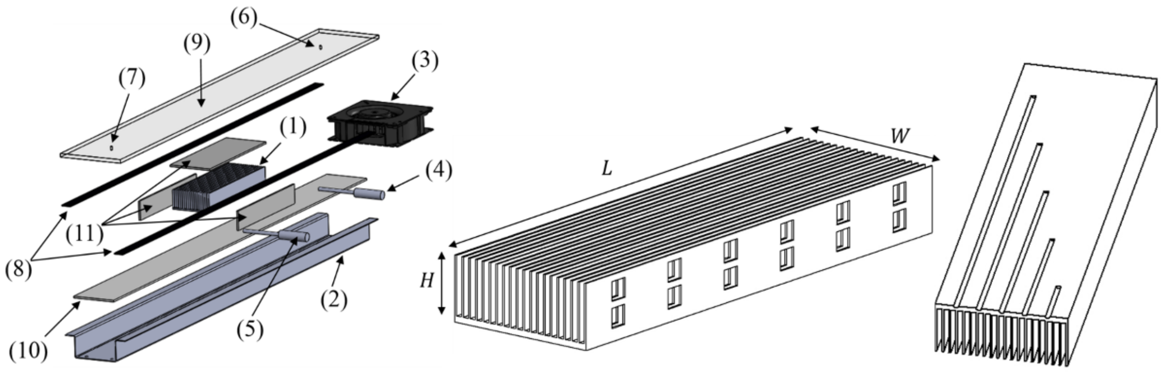

Fig. 1. [Left]: Exploded view of the experimental setup. (1): heat sink; (2): air duct; (3): blower; (4, 5): inlet and outlet resistance temperature detectors; (6, 7): high and low-pressure sensors of the differential pressure transducer; (8): rubber gasket; (9): polycarbonate cover; (10): insulation layer at the floor of the duct; (11): insulation layers around the heat sink. [Middle]: A PFHS with 12 perforations. [Right]: Bottom of heat sink.

A solid-finned heat sink (SFHS, a heat sink without perforations) was used as the base for comparisons. Five grooves at different distances from the inlet of the heat sink were machined on the heat sink base (shown in Fig. 1 [Right]). Five T-type thermocouples were inserted into grooves for measuring the temperature distribution across the heat sink base. A uniform heat load was provided to the base of the heat sinks by using a 51 mm by 203 mm insulated flexible heater that was adhered to the heat sink base. The heater was powered by a variable transformer. The duct and heat sinks were covered by thermal insulation layers to minimize the heat loss to ambient. By subtracting the sensible absorbed heat by the air from the electrical heat input, the heat losses in the present experiments ranged 3.4-7.9%. Therefore, it is assumed that the whole input heat was absorbed by the heat sink. As a result, the electrical input heat (Q) is used for data reduction. The total airflow rate inside the air duct $\left(\dot{V}, \frac{\mathrm{m}^3}{\mathrm{s}}\right)$ was determined by using an airflow bench. The Reynolds number (Re, based on the hydraulic diameter of the channel), and the thermal resistance of the heat sink $\left(R, \frac{℃}{W}\right)$ are calculated as follows:

$$\mathrm{Re} = \frac{2\rho\dot{V}}{\mu N(W_{\mathrm{ch}} + H)} \tag{2}$$

$$R = \frac{T_{b,\max} - T_i}{Q} \tag{3}$$

where N, $T_{b,\max}$ and T_i are the number of channels (=19), the maximum temperature recorded by the embedded thermocouples at the heat sink base, and the inlet temperature of the air, respectively. While thermal resistance is an important design criterion used to describe the thermal performance of a heat sink, pressure drop (ΔP) is another key design parameter, as such, a large ΔP may hinder using the heat sink regardless of its low thermal resistances. ΔP is well described by the pumping power (P_p), which is correlated as follows:

$$P_p = \dot{V} \times \Delta P \tag{4}$$

In the present experiments, ΔP across the heat sink was measured by a differential pressure transducer, which its high and low-pressure sensors are shown by numbers 6 and 7, respectively, in Fig. 1.

2. RESULTS

The maximum value of the ratio of the Grashof number to the square of the Reynolds number in the present experiments was below 6.35×10^{-4}, which indicates forced convection as the dominant mode of heat transfer [5, 6]. Fig. 2 illustrates the thermal resistances of the heat sinks as a function of the Reynolds number. Due to a negligible deviation in the air densities (below 1.3%) at a given heat load among all heat sinks, Reynolds numbers are proportional to flow rates [5]. Based on Fig. 2, although at a given Reynolds number all PFHSs reduced thermal resistances, this encouraging result without any information about ΔP across PFHSs is not persuasive enough to use PFHSs instead of the SFHS.

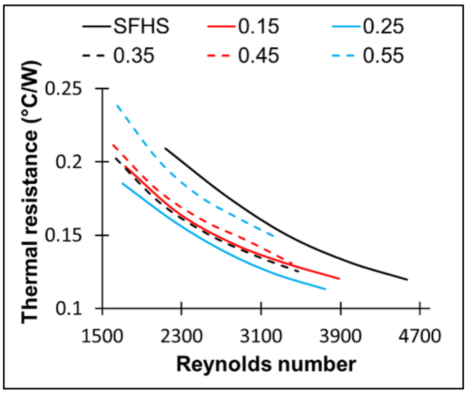

Fig. 2. Thermal resistance versus Reynolds number. Legends stand for SFHS and PFHSs with different porosities.

The pressure drops across different heat sinks are illustrated in Fig. 3. ΔP increases monotonically by increasing the number of perforations due to a monotonic increase in flow disturbances inside the channels. In addition, although increasing the porosity reduces the solid lateral surface of the fins, the pressure drops become larger monotonically, which indicates the dominance of the pressure drag compared with the friction drag in PFHSs. Comprehensive explanations can be found in [1, 5]. Although all the heat sinks were tested at the same input blower voltages, various heat sinks experienced different ranges of Reynolds numbers (flow rates), which is due to different flow resistances among heat sinks. Therefore, based on Eq (4), PFHSs are potentially appropriate thermal management solutions for reducing pumping power although they increase ΔP.

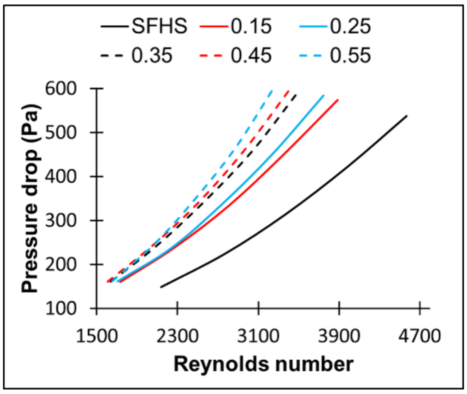

Fig. 3. Pressure drops versus Reynolds numbers. Legends stand for SFHS and PFHSs with different porosities.

While based on Fig. 2, PFHSs are promising cooling devices for reducing thermal resistances at a given flow rate/Reynolds number, Fig. 3 reveals the limitations of using PFHSs as their higher pressure drops. Here, it is necessary to describe the thermal performances of heat sinks based on the pumping power that includes the effects of both flow rates and pressure drops, as illustrated in Fig. 4. This figure provides a sufficient insight about performances of individual PFHSs as well as a valid technique for comparing thermal performances of different heat sinks with each other. Based on Fig. 4, at a given pumping power, the PFHS with the porosity of 0.25 resulted in the lowest thermal resistances among all the heat sinks tested in the present experiments, and the PFHSs with porosities at 0.15 and 0.35 came next. Also, the PFHS with $\phi = 0.45$ is an interesting design due to its negligibly higher thermal resistances, but substantially lower-weight than those of the SFHS, respectively. However, the PFHS with $\phi = 0.55$ considerably increased the thermal resistances. This is an important finding because based on Fig. 2, all PFHSs seem promising in reducing the thermal resistance at a given Reynolds number (flow rate), while Fig. 4 presents the PFHS with $\phi = 0.55$ as the low-efficient cooling device. In fact, increasing the porosity beyond a certain value leads to the deterioration of thermal performance since the majority of the conducting path of the fins are removed by perforations. Therefore, using the PFHS with $\phi = 0.55$ by relying on the results obtained from Fig. 2 would be practically unacceptable.

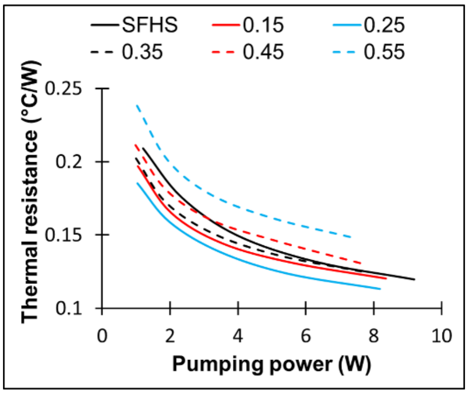

Fig. 4. Thermal resistances versus pumping powers. Legends stand for SFHS and PFHSs with different porosities.

3. CONCLUSIONS

The key role of pumping power to report thermal performances of air-cooled heat sinks was demonstrated through conducting experiments using PFHSs at different porosities. It was shown that describing the thermal performance of a heat sink as a function of Reynolds numbers without considering the effects of pressure drops across the heat sink may lead to overestimation of the overall performance of the heat sink, which is not practically acceptable. In addition, the present study introduces a new family of efficient thermal management solutions to reduce thermal resistances without any penalty in pumping powers.

ACKNOWLEDGMENT

This material is based upon work supported by the National Science Foundation under Grant# IIP-1059286 to the American Society for Engineering Education. Also, the support extended by the Office of Science in the U.S. Department of Energy, award# DE-SC0011317 is gratefully acknowledged. The author is thankful to Ms. Abbey Gall for her support to set up the experimental testbed.

REFERENCES

[1] Shaeri, M.R., Bonner, R., "Laminar forced convection heat transfer from laterally perforated-finned heat sinks," *Applied Thermal Engineering*, 116, pp. 406-418, (2017).

[2] Shaeri, M.R., Richard, B., Bonner, R., "Cooling Performances of Perforated-Finned Heat Sinks," *ASME Heat Transfer Summer Conference*, pp. V001T05A005, Washington, DC, USA, July 10-14, (2016).

[3] Staats, W.L., "Active heat transfer enhancement in integrated fan heat sinks," *PhD diss., Massachusetts Institute of Technology*, (2012).

[4] Bar-Cohen, A., Iyengar, M., "Design and optimization of air-cooled heat sinks for sustainable development," Thermal Challenges in Next Generation Electronic Systems, Joshi & Garimella (eds), Millpress, Rotterdam, pp. 5-21, (2002).

[5] Shaeri, M.R., Bonner, R., "Heat transfer and pressure drop in laterally perforated-finned heat sinks across different flow regimes," *International Communications in Heat and Mass Transfer*, 87, pp. 220-227, (2017).

[6] Yaghoubi, M., Shaeri, M.R., Jafarpur, K., "Three-dimensional numerical laminar convection heat transfer around lateral perforated fins," *Computational Thermal Sciences*, 1, pp. 323-340, (2009).